Journal of Autonomous Intelligence (2023) Volume 6 Issue 3
doi: 10.32629/jai.v6i3.795

ORIGINAL RESEARCH ARTICLE

A shadow preservation framework for effective content-aware image retargeting process

Ankit Garg[1,2,*], Aleem Ali[3], Puneet Kumar[3]

[1] *Apex Institute of Technology (CSE), Chandigarh University, Mohali 140413, Punjab, India*
[2] *University Centre for Research and Development (UCRD), Chandigarh University, Mohali 140413, Punjab, India*
[3] *Department of CSE, University Institute of Engineering, Chandigarh University, Mohali 140413, Punjab, India*
*** Corresponding author:** Ankit Garg, ankitgitm@gmail.com

ABSTRACT

In the discipline of image retargeting, the structure of shadows in the image is required to be preserved since it gives structural information about the objects. Many traditional image retargeting techniques do not pay attention to preserve the shadow objects present in the image. In this paper a shadow-preservation framework is proposed in which the saliency map is derived using segmentation-based gPb-owt-ucm approach to emphasize the salient regions. To assess the quality of saliency map a fixation prediction analysis is conducted on each section of the image using the eye tracker technology. Second, to pay more attention on the shadow objects a shadow map is developed after executing image pre-processing, shadow detection, region growing, and region filling operations. To rectify the issue of misclassification of shadow pixels erosion and dilation operations are performed. To obtain an efficient importance map, a gradient map is prepared using canny operator which is further combined with the saliency map and shadow map. The obtained importance map is supplied to the seam diversion based image retargeting (SDIR) technique to resize the image in horizontal and vertical directions. To justify the efficiency of the proposed framework's the obtained results are compared with the existing state-of-the-art. By preserving shadows, the proposed framework enhances the overall visual quality and maintains the integrity of objects in the retargeted images. The framework's effectiveness is validated through quantitative evaluations and visual comparisons with existing methods. The results demonstrate its potential for improving content-aware image retargeting applications, paving the way for more realistic and visually appealing image resizing techniques in various domains.

Keywords: content-aware; image resizing; retargeting; seam carving; saliency map; shadow map; segmentation; warping; Multi-operator

ARTICLE INFO

Received: 11 July 2023
Accepted: 14 August 2023
Available online: 18 September 2023

1. Introduction

Nowadays different types of multimedia contents are being shown on different online software. The web browsers are presenting dynamic multimedia contents which change itself time to time. The user can visualize continuously change in the aspect ratio of the image while surfing on the Internet. Therefore, image retargeting process is very critical in image browsing and web browsing applications. In recent years, content-aware image retargeting techniques have been used to keep important elements intact in an image while scaling it. The recognition of salient areas from images during the image retargeting process is a time-consuming procedure. As a result, several improved saliency detection algorithms are utilized to extract regions of interest (ROI). The image resizing process is completed in two steps: (i) identifying the salient sections of the image, and (ii) implementing an effective resizing approach. Several image resizing methods are now

extensively utilized, including scaling, cropping, seam carving (SC), patch-based technique, warping, and Multi-operator (Multi-Op)[1]. Image ROI are the regions that attract human visual attention and include low and high-level image object properties.

Every image retargeting algorithm has the goal of preserving the structural loss of prominent areas while image retargeting. Gradient energy, image frequency, contrast, and color characteristics are examples of low-level image properties. Faces, people, and things might be regarded significant features of image objects in the case of high-level features. The image's saliency map may be generated by taking into consideration the image's low and high-level characteristics. In order to create a basic saliency map, the gradient approach is often used. The saliency map records the intensity fluctuation between image pixels in order to emphasize the most significant locations. Because of its simplicity and low processing time, the gradient approach is most typically used in the operation of saliency detection or the development of an image's energy map. A temporal saliency map is constructed by detecting pixels that shift differently by evaluating optical flow or motion vectors. Importance maps with movement and image depth saliency are used for stereoscopic video. To assess saliency, the bottom-up approach employs pixel intensities, edge orientation, and pixel color.

Top-down techniques leverage semantic data contained in an image, such as the position of important things (e.g., text, bodies, faces), as well as symmetries. In the realm of image retargeting, both top-down and bottom-up methodologies may be employed to evaluate image saliency. Some earlier foreground models focused on obtaining high edge values for an image while neglecting low values within an item's interior. Wei et al.[2] proposed a methodology for extracting background information based on past knowledge. The model compares all pixel deviations at backgrounds. Itti et al.[3] proposed a method for estimating bottom-up saliency that is promoted by the human visual system by concentrating on the low-level properties of image objects. The proposed method uses a pyramid methodology to generate three distinct saliency maps. Texture, direction, and intensity are the low-level characteristics examined throughout the estimate. Ultimately, the feature maps that have been found are combined to create a single saliency map. Stentiford[4] proposed a technique for estimating image saliency based on severe fluctuations among nearby pixels in the image. As compared to Itti et al.'s method, the recommended approach is more efficient. It can make the image's prominent sections wider and smoother.

Santella et al.[5] suggested a method for cropping images that makes use of an eye-tracking device to detect the most conspicuous ROI in the image. Gal et al.[6] and Golub[7] developed a method for estimating ROI. Manual computation is necessary in this technique to estimate the prominent points in the image. To avoid disappointing findings from automatic algorithms, the relevance map of an image can be explicitly specified in the literature[8,9]. Although researchers have presented numerous saliency detection approaches, many enhancements are still required to extract an appropriate significance map when the image includes the shadows of the objects portrayed. The majority of saliency detection algorithms identify the shadow as a minor element of the image or background item. When an image retargeting operation is done on the image, the ideal seams encompass the region that the objects put in shadow. The elimination of pixels from the shadow area may result in severe data lost.

The shadows of the items are also significant in recognizing and comprehending the architecture of the objects, such as the depth of the image contents, the direction of the incoming light, and the object's distinctiveness. The removal of the shadows of noticeable objects may result in a distortion of the structural and visual presentation of the items in the image. For example, an item's shadow can be precisely measured; nevertheless, the shadow may not suit the form of the object; hence, under equal lighting circumstances, one object has a shadow while the other does not. Several more instances may be discovered while retargeting shadowed images. After completing multiple investigations, the researchers concluded that shadow objects may also be seen as image informative material that leads the human attention to the image's principal

components. The existence of shadows allows the spectator to understand crucial information such as the strength of incidence light on the object, the depth of the object, the direction of the incoming light, and other critical aspects of the items. As a result, keeping the object's shadow when retargeting photographs is crucial.

SC, one of various image retargeting techniques, is being employed in image forgery detection. Researchers have proposed many models that are employed in the healthcare industry[10–12]. In health care sectors image retargeting techniques can be used to reduce the size of the high resolution image so that they can stored effectively in healthcare database. The proposed significance map may be implemented into the proposed models to determine the key parts of the images in order to accurately recognize the damaged section of the body.

2. Literature review

In this section, a literature review on existing image retargeting operators is presented that includes facts, findings, and improvement methods suggested by the researchers. In this literature review, 7 well-known categories of image retargeting have been presented such as Cropping, Scaling, SC, Shift-Map (SM), Scale and Stretch (SNS), Warping, and Multi-Op.

Cropping is a fairly old image retargeting method that involves placing a square cropping window in the center of the image. The window-captured section of the image stays intact, but the region just outside of the window is cropped out. The precise placement of the window in the cropping strategy is a difficult issue. Chen et al.[13] proposed an automated cropping approach that combines focus preservation and region cropping. Kao et al.[14] proposed a visually attractive map-based cropping approach. An aesthetic map based on the aesthetic quality category may be used to separate the image regions. The gradient energy map is employed to illustrate the geographic distribution of the image's notable edges. Two maps are used to examine the quality of the composition and related model: aesthetic and gradient energy maps. For image cropping, Guo et al.[15] suggested a cascaded cropping regression technique. To address the issue of a lack of labelled cropping data, the proposed technique adopts a two-step learning process. To solve the challenge, a classifier is trained using a Convolution Neural Network (CNN). It is then meant to obtain cropping properties from a database. Several images are trained with a deep learning approach devised by Rahman et al.[16] to build accurate significance maps via graph-based segmentation and ray level modification. A Gaussian filter is employed to detect the prominent components in the image. The suggested framework's major goal is to safeguard the image's significant features.

The typical scaling method causes the image's structural information to be lost. When real-time applications are used to display the image contents, the scaling strategy also creates aliasing[17]. The observer frequently notices the aliasing effect when there is a large difference in display size between the input and output images. Jiang et al.[18] proposed an efficient edge-adaptive scaling method capable of dividing the original image into four distinct kinds of image blocks. Following that, interpolation is performed to the image in the orientation of the conspicuous edges. Liang et al.[19] suggested a patch-wise scaling approach effective for preserving image ROI while also reducing overall visual artefacts caused during the image scaling process. Pritch et al.[20] proposed a novel technique which deals with geometric changes in images, such as resizing, inpainting, and object repositioning. These changes are defined by a shift map, indicating pixel shifts from input to output. The method introduces a fresh way to represent these operations using optimal graph labeling. This involves assigning labels to output pixels based on the shift map. Avidan and Shamir[21] suggested a content-aware image retargeting strategy that protects the image's important sections when retargeting. The best seams are constructed to locate the image's lowest energy pixels in both horizontal and vertical orientations. The gradient method is typically employed to produce the image's energy map. Dynamic programming is used to produce ideal seams at various positions in the image. Choi and Kim[22] proposed a

modified effective seam-carving approach that can keep the image's salient region while also retaining the image's essential structure that is visible to the human eye. The recommended approach calls for ideal seams to be allocated to each other sparingly. Lin et al.[23] proposed a saliency-based seam-carving approach. The proposed method categorizes images using the greyscale of detection and localization. Following the calculation of the cumulative energy map, the foreground and detailed regions can be safeguarded by integrating multiple protection strategies. To remove single-pixel wide seams, the approach of deleting the least energy pixel is applied.

Li et al.[24] proposed a SC approach that makes use of unideal and discontinuous seams. By enabling optimum seams to travel in homogeneous regions of the image, spatial-temporal coherence may be retained. A genetic algorithm is used to reduce processing complexity. Each frame may be extended to the required size by eliminating the seams one at a time. Patel and Raman[25] proposed a method for effective SC based on numerous pixel-wide optimum seams. The proposed method inserts and removes numerous least energy pixels in a single cycle. The energy of pixels is intentionally added to prevent the production of spurious edges. The thickness of a multiple-pixel seam is an essential part that may be modified based on the user's requirements. Researchers have made substantial contributions to improving the standard SC technique by employing energy improvement and seam diversion procedures[26–28]. Warping-based image retargeting strategies are ongoing approaches for creating retargeted images. The warping approach's goal is to retain the image's most visible portions while producing considerable distortion in the image's least visible sections. To achieve smoother image retargeting results, researchers offered many retargeting algorithms that focused on distinct limitations and optimization methodologies. Kaufmann et al.[29] proposed an efficient retargeting system that employs a finite element technique to achieve warping. Li et al.[30] suggested a warping-based stereo image retargeting approach that protects image object spatial features as well as the depth of 3D sceneries. To estimate the computed depth distortion, use the integrated warping function. Del Gallego and Ilao[31] proposed an SR system based mostly on smart phones. The proposed method employs a classic multiple-image super-resolution (SR) method that makes use of low-resolution images recorded by a camera. To regain the 3D visual experience, Islam et al.[32] presented a warping-based approach for retargeting and remapping the depth of stereoscopic video. Niu et al.[33] proposed a novel method for resizing images to different display sizes while preserving global structure and minimizing distortion. It handles both large and small displays with specialized strategies, utilizing quadratic metrics and a patch-linking approach. The resizing process is framed as a quadratic minimization problem for efficient resolution. Experimental results demonstrate its superiority over existing techniques across various image categories. Wang et al.[34] presented a "scale-and-stretch" image resizing technique that preserves key features by optimizing local scaling factors and using a significance map to control distortion in uniform areas, ensuring minimal impact on important elements. This approach distributes distortion in all directions, even for horizontal or vertical resizing, and supports interactive resizing.

Image retargeting with a single operator is insufficient to create attractive retargeting outcomes. To create a hybrid sequence, various image retargeting operators must be integrated. Rubinstein et al.[35] proposed an algorithm that optimally combines resizing operators. The proposed technique introduced a resizing space, where paths represent retargeting operations, using a unique image similarity measure called Bi-Directional Warping (BDW). The proposed approach extends to videos with key-frames and interpolation, offering flexible operator combinations throughout the sequence. Su et al.[36] suggested a multiple operator retargeting approach that involves Cropping, SC, and Scaling. In the proposed method, all of the operators are used on the image in a preset order to provide visually acceptable retargeted outcomes. The switching point is introduced among the operators to acquire their benefits when retargeting the photos. Tsai and Chen[37] proposed an image retargeting method that begins with a cropping operator. If the dimension of the retargeted image is not the required image size, an aspect ratio correction procedure is used. Lastly, the retargeted result is obtained using

a uniform scaling operator. Zhu et al.[38] suggested a Multi-Op image retargeting method that maintains image structural loss. The proposed approach classifies images that use SIFT density. The proposed approach improves the performance of the image retargeting operators described in the hybrid sequence by utilizing the Earth Mover's Distance and Gray-Level Co-occurrence Matrix ideas. To enhance the image retargeting process, Garg and Negi[39] suggested a Multi-Op image retargeting approach that includes Cropping, Warping, and SC techniques. An optimized function that integrates IMED (Image Euclidian Distance) and DCD (Dominant Color Descriptor) is utilized to evaluate the effectiveness of the suggested method.

Karni et al.[40] proposed flexible energy-based method for shape deformation, applied to image resizing and 2D shape changes. The proposed energy approach accommodates a wide range of valid transformations efficiently. This flexibility ensures natural and minimally distorted results in image and shape manipulation, while also reducing unwanted foldovers and self-intersections. Chen et al.[41] introduced a novel approach for content-aware image resizing using a global optimization framework. The proposed method reveals that the core resizing challenge can be represented as a convex quadratic program. Moreover, the proposed method extends this framework to avoid mesh foldovers, amplify important areas, and retain straight lines. The efficiency of the proposed algorithm is showcased through comparisons with state-of-the-arts. Shi et al.[42] introduced an innovative technique to manage the size of prominent objects during image resizing. By adjusting a single parameter, this method lets users modify the main object size according to their preference. To achieve this, a fresh quad distortion energy criterion is presented, factoring in both quad shape and size. Additionally, the single resolution visual attention model is enhanced into a multi-resolution saliency model by considering feature rarity. The significance map is redefined as a weighted average of this multi-resolution saliency outcome and gradient magnitude.

3. Proposed framework

3.1. Description of the proposed framework

The aspect ratio of the source RBG image can be altered through the existing SDIR algorithm[26] by utilizing the proposed importance map.

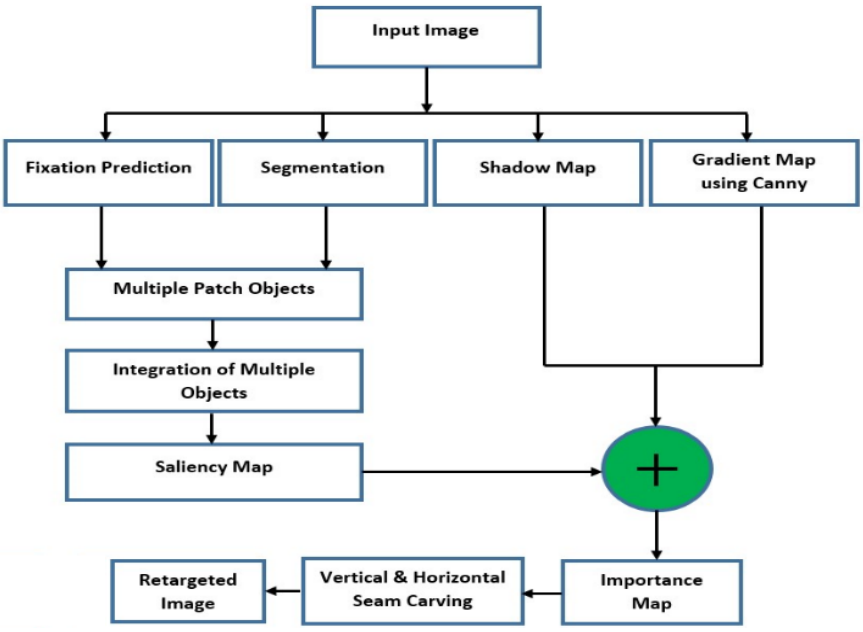

Figure 1. Proposed shadow preservation framework.

The saliency map's key benefit is that it represents the conspicuous objects; the shadow map may be used

to provide details of the shadow patterns; and the gradient map derived from the Canny operator is used to provide details of the prominent edges. The proper computation and integration of several maps can emphasize the most prominent parts in the image and be used in the SDIR technique to create distortion-free retargeted images. **Figure 1** depicts the suggested shadow preservative framework's procedure.

3.2. Computation of saliency map based on segmentation

The image's saliency map illustrates the ROI that must be retained while retargeting the images. The ROI of an image reflects the major portions of the image that capture the viewer's attention. Bottom-up and top-down techniques can be used in the area of detection and localization. These methods detect the salient regions using visual attributes such as color, intensity, and direction, as well as semantic information.

Computation of saliency map

The segmentation-based gPb-owt-ucm[43] approach is used to construct an efficient saliency map. **Figure 2** shows the process of saliency detection using segmentation. Following segmentation, three characteristics, namely centricity, border ratio, and boundary ratio of each segmented patch, are determined to determine the saliency of each partitioned block of pixels. To begin, the distance between the centre of the segmented patch and the centre of the entire image is determined in order to compute the centricity of distinct segmented patches of the image. To begin, centricity refers to the distance between the center of a segmented block of pixels and the center of the input image. Patches closer to the image's center are awarded a greater saliency rating. The center of the segmented patch can be represented by (x_c^k, y_c^k). To compute the normalized center $N_c^k = (\frac{x_c^k}{h}, \frac{y_c^k}{w})$ can be used, where h and w denotes the height and width of the image respectively. The saliency value of the segmented patch k which is based on centricity can be obtained using Equation (1). In Equation (1), I_c is the center of the image.

$$S_c^i = 1 - \left\| N_c^k - I_c \right\| \tag{1}$$

Secondly, border based saliency of segmented image patch k can be defined using Equation (2), where NB_s^i and NB_{Im} represent the number of intersection between boundary and border pixel set of image segment and whole image respectively. To identify the important salient regions of the image a border ratio is defined, the regions with higher border ratio are considered as background regions. The regions with the minimum value of border ratio are considered in the most significant regions of the image. The border set of pixels in the whole image can be obtained using, $NB_{Im}^i = 2(w + h)$.

$$S_{b0}^i = 1 - \frac{NB_s^i}{NB_{Im}} \tag{2}$$

Thirdly, to compute the boundary ratio S_{b1}^i a ratio between boundary pixels of image segment k and count of intersection between boundary and border pixel set of image segment and whole image. The regions with higher boundary ratio are considered in the most significant region of the image. A region can be considered as a less prominent area of the image if the value of the boundary ratio is high. Based on the saliency of segment k the boundary ratio can be defined by Equation (3), where NB_s^i represent the set of pixels lie on the boundary of segment k.

$$S_{b1}^i = 1 - \frac{NB_s^i}{NS_{Im}} \tag{3}$$

To obtain the level of the saliency correspond to each segment above three properties are combined. Equation (4) is used to obtain the final result of the saliency level of each segment k.

$$S_i^k = \prod_{j \in \{c, b_0, b_1\}} S_j^k \tag{4}$$

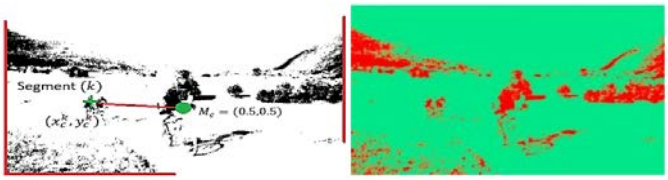

Figure 2. Saliency detection. **(a)** image segmentation. The green spot inside the image shows the center of the image and the red line shows its distance from a segment *k*. The red lines on the border of the image represent the overlapping of boundary and border pixels of the segment and image; **(b)** ROIs are labeled[44].

4. Evaluation measures for saliency map

To assess the quality of the saliency map, quantitative analysis is performed. The resulting saliency map may be visually examined and contrasted with the state of the arts in the given datasets in the qualitative analysis. Fixation prediction analysis is conducted on each section of the image using the eye tracker technology for qualitative assessment of the saliency map. The fixation prediction analysis results provide a quantitative description of the eye movement behavior. The saliency threshold in this analysis is determined by the density of fixation sites depending on fixation time. To study the visual focus on a particular region in an image, 50 shots were taken in a random way, and the length of stable gaze is estimated for around 250–350 milliseconds. Eventually, the findings of several sections are integrated to create a hierarchy of salient objects based on eye fixations and segmentation. **Figure 3** depicts the methodology for creating the saliency map using the RetargetMe dataset[45].

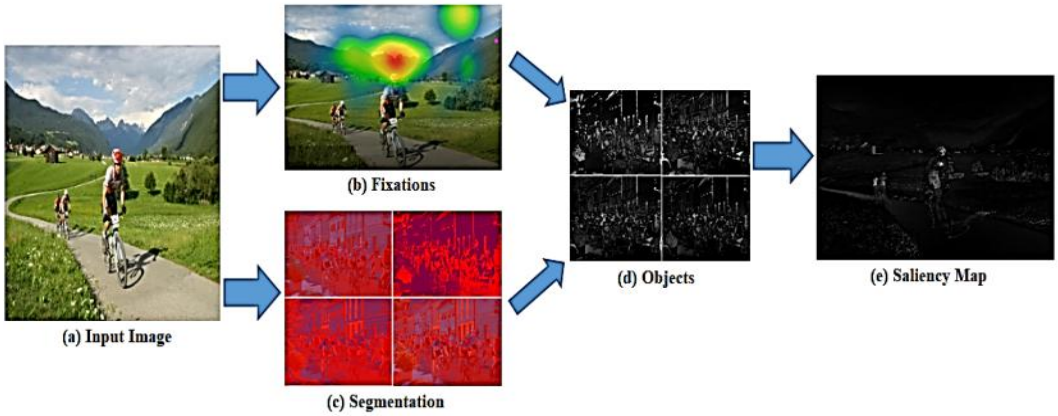

Figure 3. Framework for constructing the dataset using recorded fixation points[44].

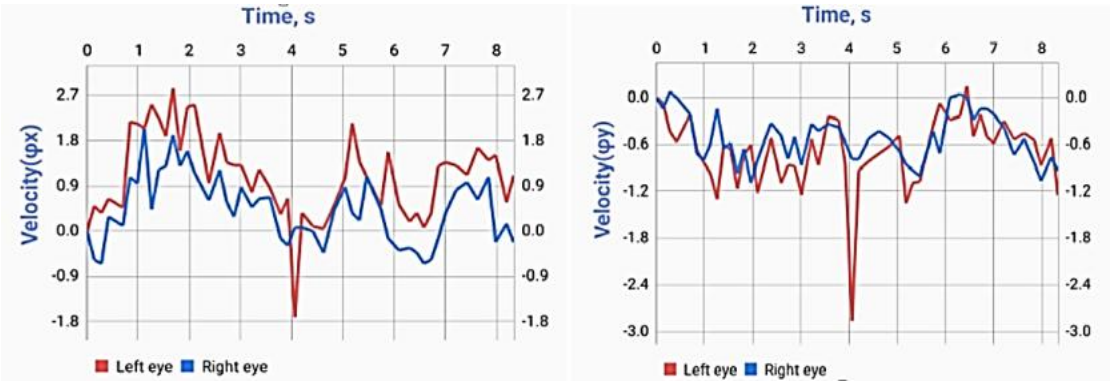

Figure 4. Results of the metrics of a saccadic eye movement.

The image containing the shadow areas is chosen and loaded into the video eye-tracker recording device. The video eye-tracker equipment has been setup with various parameters namely cam field of view vertical 180, pupil distance 720.16 mm, and calibration type 5 points, which detect distinct fixation sites from the

image. The red curve shows the position of fixation targets, while the blue curve represents the position of the fovea in both the horizontal and vertical directions, as shown in **Figure 4**. To better assess motion, the speed data of changes random direction has been incorporated. The resultant saliency map is compared to state of the arts recorded in the accessible datasets for quantitative analysis. The RetargetMe dataset, which contains 500 images and their ground truth, is utilized as a comparison. Moreover, using the binarization procedure, the saliency map is transformed to a binary mask (B), which is then compared to the known ground truth (GT) to calculate the *Precision* and *Recall* values using Equation (5).

$$Precision = \frac{|B \cap G|}{|B|}, Recall = \frac{|B \cap G|}{|GT|} \tag{5}$$

To perform the binarization on the obtained saliency map, image dependent adaptive-threshold is used to compute the mean saliency of saliency map S.

$$T_a = \frac{2}{W \times H} \sum_{x=1}^{W} \sum_{y=1}^{H} S(x, y) \tag{6}$$

In Equation (6), height and width of the obtained saliency map can be represented by H and W respectively. According to available literature existing measures to assess the quality of binary mask do not generate the appropriate result of the evaluation. To get the reliable performance evaluation results a new weighted F-measure measure is employed[46].

$$F_\beta^\omega = (1 + \beta^2) \frac{Pricision^\omega . Recall^\omega}{\beta^2 . Pricision^\omega + Recall^\omega} \tag{7}$$

In Equation (7), β denotes the efficiency of detection.

5. Shadow map extraction

The saliency map produced from the image is important in delivering visually appealing retargeted outcomes in the content-aware image retargeting approach. Yet, according to the literature, researchers have proposed numerous ways for generating the saliency map of an image without taking into account the shadow of the image objects. The suggested framework extracts the image's shadow map by employing image pre-processing, shadow detection, and region filling. The resultant shadow map is blended with the acquired gradient map through the canny operator. Ultimately, the three separate maps are blended to form the image's significance map.

5.1. Proposed shadow detection model

Figure 5 shows the proposed model to generate the shadow map of the input RGB image. The proposed model has three main stages namely pre-processing stage, the process of shadow detection, and region filling process using image morphological operations.

After performing all the operations, the shadow map is generated which is combined with the obtained saliency map to generate an accurate importance map. The importance map generated in this way considers the shadow of the image objects as prominent structures that should be preserved while retargeting the images.

In **Figure 6**, the various stages in image pre-processing are shown. Initially from RGB image three main components or color spaces such as c_3, saturation (S), and intensity (I) are computed. The RGB model is transformed in to the HSI color model, after that c_1, c_2, c_3 color spaces are obtained after manipulation of RGB color model.

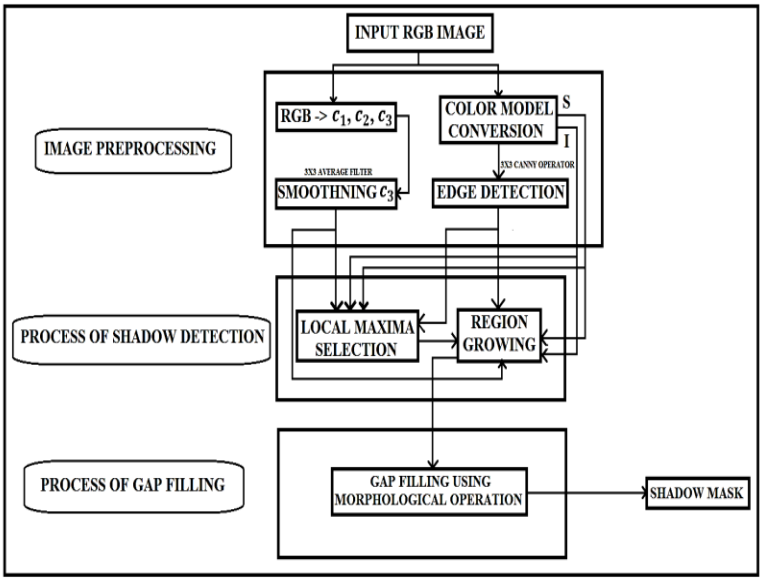

Figure 5. Framework for generating shadow mask.

For computing c_1, c_2, c_3 color space Equations (8)–(10) are used.

$$c_1(R,G,B) = arctan\frac{R}{max\{G,B\}} \tag{8}$$

$$c_2(R,G,B) = arctan\frac{G}{max\{R,B\}} \tag{9}$$

$$c_3(R,G,B) = arctan\frac{B}{max\{R,G\}} \tag{10}$$

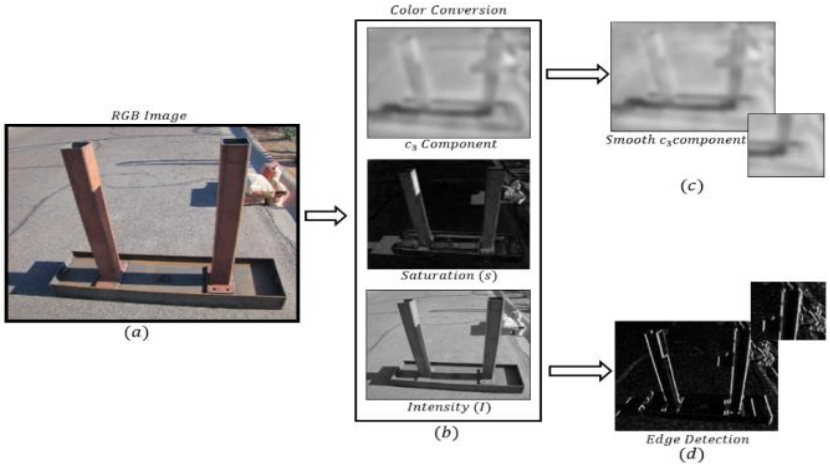

Figure 6. (a) input RGB image; **(b)** computed color components; **(c)** smoothing of c_3 component using canny operator; **(d)** computation of magnitude of the gradient[47].

After testing different images in the SBU-shadow dataset[46] c_3 band found suitable for detecting the shadow regions present in the image. In testing, it is observed that the c_3 component can be noisy, which may lead to confusion between pixels that lie under shadow and non-shadow regions. To rectify this issue c_3 component is convolved with the 3 × 3 average filter to reduce the effect of noise. To obtain the HSI components from the image Equations (11)–(14) are used. To detect the edges a 3 × 3 canny edge detector operator is applied that calculates the gradient magnitude of the image.

$$\theta = \cos^{-1}\left\{\frac{\frac{1}{2}[(R-G)+(R-G)]}{[(R-G)^2+(R-B)+(G-B)]^{1/2}}\right\} \tag{11}$$

$$H(Hue) = \begin{cases} \theta & if\ B \le G \\ 360-\theta & if\ B > G \end{cases} \tag{12}$$

$$S(Saturation) = 1 - \frac{3}{R+G+B}[\min(R,G,B)] \tag{13}$$

$$I(Intensity) = \frac{1}{3}(R+G+B) \tag{14}$$

5.2. Process of shadow map extraction

In the shadow map extraction, three main processes have been performed: (1) seed selection and shadow map extraction, (2) region growing, (3) gap filling. In the seed selection and shadow map extraction process, the initial seed is selected using the automatic seed selection process. After that, the shadow is segmented into a small region based on an obtained initial seed. To minimize the problem of over segmentation the N-cut method is applied. In the region-growing process, the neighboring pixels are added to the region recursively. The initial seeds are selected in such a way that at least one seed must be considered for each shadow region. The seed can be a group of 4 × 4 pixels. The seed matrix is placed on the pixels of c_3 smoothed band. The following steps are followed for the region growing process.

1) Let $k_1, k_2, k_3 \ldots\ldots k_i$ are the initial seed and R_i denote the corresponding region to k_i. The initial seed is selected if it satisfies the $L(x,y) > T_1$ and $Dis_{max} < T_2$. Here, $L(x,y)$ is the similarity of a pixel to its nearby pixels, T_1 and T_2 are the thresholds that minimize the ratio between class variance and within class variance. Dis_{max} is the relative distance between pixel to its neighborhood. The pixel is considered as the seed pixel if it satisfied $L(x,y) > T_1$ and $Dis_{max} < T_2$.

2) After assigning the labels to each seed region, every seed region is traversed to maintain a non-ascending order sorted list, to store the neighbor of seed areas.

3) If the list is non-empty, take the first point from the list and check all its 4 neighbors.

4) The level of P will remain the same if all its neighbor has the same label otherwise Euclidean distance of P to its neighboring regions is calculated using Equation (15).

$$d_{ij} = \frac{\sqrt{(H_i - H_j)^2 + (S_i - S_j)^2 + (I_i - I_j)^2}}{\sqrt{H_i^2 + S_i^2 + I_i^2}} \tag{15}$$

1) The mean of the region is updated and 4 neighborhoods of P will be added to the list M, which are not classified and are the neighbor of the region R_i.

2) From the obtained segmentation outcome a weighted graph $G = (V, E)$ is used to calculate the weight of the edge and the obtained information can be summarized in terms of E and D.

$$(D - E)x = \lambda Dx \tag{16}$$

here, D is a diagonal matrix, x is the Eigenvector with the second smallest value. The regions are decided based on the value of x.

3) The graph is bi-partitioned based on the second smallest Eigen value. The split point is obtained where N-cut is minimum.

4) Finally, when the total count of the elements of a segmented region is more than the $Area_{min}$ value again weighted graph is used to obtain the weight of every edge and to summarize the information.

After performing steps (1–8), the shadow map is extracted. For smoothing boundaries of obtained shadow map image morphological operations are performed.

In **Figure 7**, the outcome of the region-growing process and gap-filling operation has been shown. After performing the region-growing operation, the detected shadow regions may contain small gaps due to the misclassification of shadow pixels (true negatives). To rectify this issue a sequence of image morphological operations is performed over the obtained shadow image. To perform erosion and dilation operation a 4-pixel wide structuring element is applied over the binary shadow image.

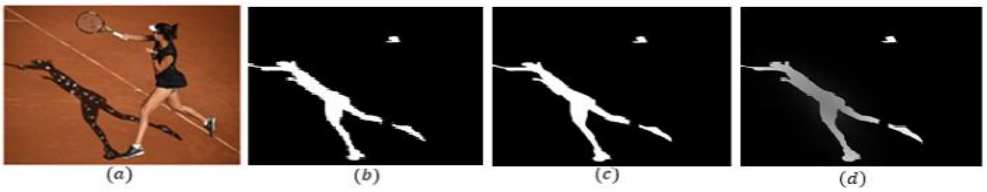

Figure 7. (a) identified seeds in the seed selection process; **(b)** shadow regions obtained using region growing operation; **(c)** gap-filling operation using dilation followed by erosion; **(d)** shadow map[47].

6. Generation of importance map for image retargeting

Figure 8 depicts the integration of many maps. To determine the saliency of each segmented patch, the saliency map produced from segmentation and three attributes such as centricity, border ratio, and boundary ratio are specified.

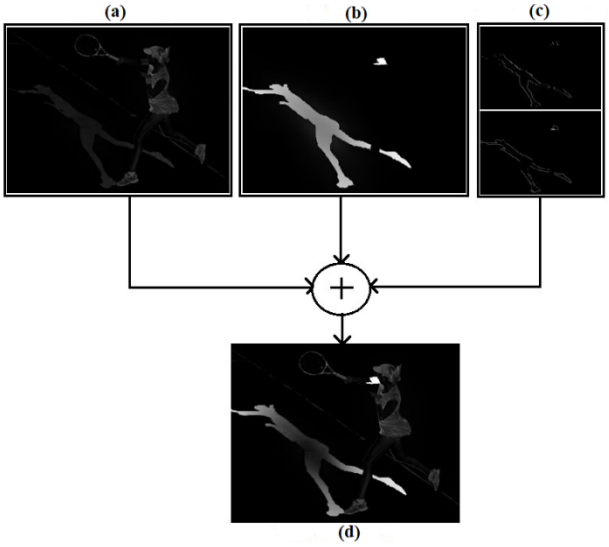

Figure 8. Integration of different maps. **(a)** saliency map based on segmentation; **(b)** shadow map; **(c)** energy map in the horizontal and vertical direction; **(d)** importance map after integration.

The aforementioned three attributes are used to compute the saliency level of each segmented image block. After applying several image processing processes to acquire the boundaries of the prominent objects and the shadow areas, the generated shadow map detects the shadow regions and raises the energy of related pixels. Edge detection is carried out in both the horizontal and vertical planes to identify the most noticeable edges that must be kept during the retargeting procedure. The graphic shows that the energy level of the salient objects and shadow areas has grown in the produced significance map. After incorporating the significance map into the SDIR technique, the optimal seams disregard the pixels in these places and skip the seams to surrounding regions where the energy of the pixels is relatively low. As a result, the image's salient structures can be retained from distortion.

7. Results & discussion

Many available image datasets can be utilized to compare the results obtained from the existing state of the art and the existing SC image retargeting techniques. From these datasets, different types of images can be chosen that contain different features of image objects. For comparison of results, the SBU-shadow dataset is used in which various images having shadows are categorized based on the indoor and outdoor environment. It is a large-scale dataset labeled using lazy annotation and contains 638 testing images. The dataset contains images that cover a large range of scenarios, such as beach, mountain, road, and snow. The another reason of selection of SBU dataset is less annotation errors as compared to other existing datasets[48]. From the available images in the dataset, it can be observed that shadow preservation in the outdoor scene is relatively more difficult than the indoor scenes in which various issues can be considered such as overlapping of multiple shadows, noisy background, and change of illumination, etc. For the testing and verification of the proposed scheme, five categories of images have been considered which are given below.

- Category 1: Shadow on the surface where the variation of intensity is very low.
- Category 2: Shadow covers a large portion of other objects present in the image.
- Category 3: Overlapping of shadows.
- Category 4: Shadow overlaps prominent line structures.
- Category 5: An outdoor environment where the only shadow is available as a prominent region of the image.

Image distortion can be easily analyzed on 5 categories of images during the image retargeting process. In the following sections, the achieved findings are shown and described.

7.1. Comparisons

The findings of the proposed framework are reviewed after integrating the proposed importance map with the present SC algorithm to analyze the improvement of the existing SC algorithm. The results of the proposed framework are compared with five cutting-edge image retargeting techniques: SM[20], SC[21], Warping[33], SNS[34], and Multi-Op[49]. Because of the benefits of reduced distortion and lower time consumption, these techniques are commonly employed in image processing applications. One of the most successful retargeting tactics available today is the Multi-Op strategy. **Figure 9** illustrates the original or input photographs that were utilized for testing and comparing the results obtained from the proposed framework. The suggested framework seeks to keep the notable characteristics of the salient objects with shadow areas while retargeting the images.

Figure 9. Input images[47].

1) Category 1

Figure 10 depicts the outcomes of all five cutting-edge approaches for producing shadow distortion on the pool's water or its bottom. The noticeable structure of shadow is deformed in all state-of-the-art after seams are removed from the image. The suggested shadow preserving framework, when combined with the existing SDIR technique, yields the best results that are both aesthetically appealing and less deformed. The distortions

are not clearly observed from the naked eye since the majority of the seams cover areas with relatively modest energy fluctuations. The suggested significance map boosts the energy of the important items and the part of the image that is under shadow. The SDIR approach selects nearby pixels with the least amount of energy and the best seams to avoid the salient objects and shadow regions indicated by the suggested significance map. While retargeting images, the suggested framework creates less distortion when compared to existing techniques. Also, the suggested framework protects the aspect ratio of important regions in the image, which is a drawback of existing retargeting systems. When the visual contents of the images are examined, it is discovered that SNS and Multi-Op usually change the structure of the shadows and other major elements of the image.

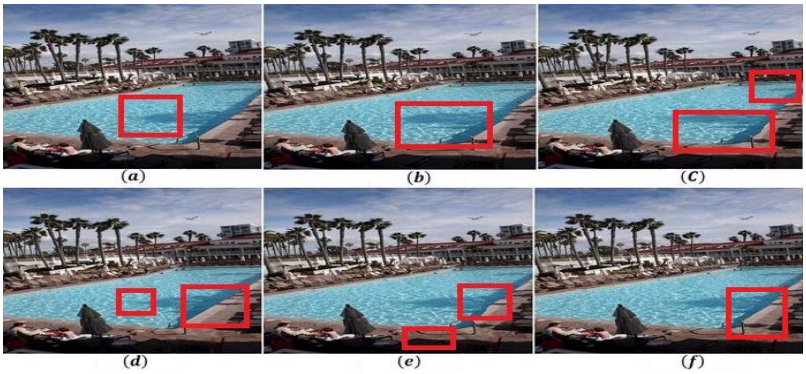

Figure 10. (a) SC; **(b)** SM; **(c)** SNS; **(d)** Warp; **(e)** Multi-Op; **(f)** proposed[47].

In comparison to SNS and Multi-Op techniques, the other methods considered, notably SC, Warp, and SNS, produce fewer distortions. The suggested method works effectively and produces high-quality results with minimal structural degradation on visible objects. The suggested approach produces deformations that are difficult to identify with the naked eyes of the observer.

2) Category 2

From **Figure 11**, it is observed that the edges of the building and shadow of the tree are highly distorted in the case of Warp and Multi-Op image retargeting operators. The distortion percentage of SNS is higher than SM, SC, and the proposed framework. Although, the percentage of distortion obtained from SC is less. The deformations produces by SC can be easily noticeable to the human visual system. In this category of image type, proposed framework performs well and produces fewer distortions that are not easily noticeable.

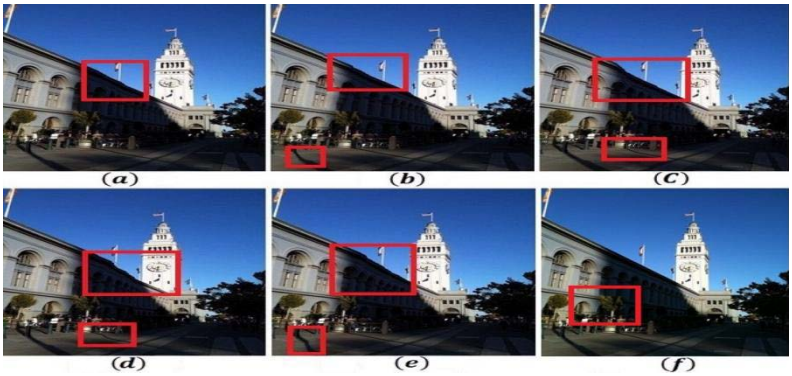

Figure 11. (a) SC; **(b)** SM; **(c)** SNS; **(d)** Warp; **(e)** Multi-Op; **(f)** proposed[47].

3) Category 3

From **Figure 12**, it is obvious that SM and Multi-Op provide outcomes that are almost identical. As compared to the SM, Multi-Op, and SDIR schemes, SC and SNS yield a significant amount of distortion.

Among all image retargeting operators, Warp has the highest percentage distortion. The suggested method performs effectively for this category of image type and causes relatively few distortions that are not immediately visible to the human eye.

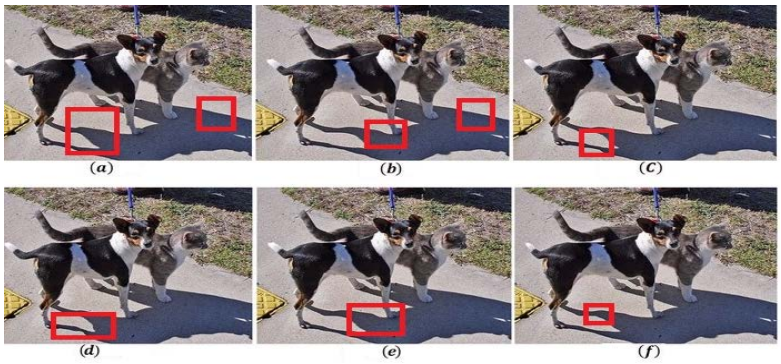

Figure 12. (a) SC; **(b)** SM; **(c)** SNS; **(d)** Warp; **(e)** Multi-Op; **(f)** proposed[47].

4) Category 4

The deformation of line segments and shadow regions in the results can be seen in **Figure 13**. The current state-of-the-art causes distortions across line structures and shadow areas. The greatest level of distortion can be seen when the Warp and Multi-Op image retargeting operator is applied. SC and SNS provide nearly identical outcomes. SNS also causes distortions in line structures that are visible to the naked eye. In this image category, the proposed framework outperforms traditional image retargeting techniques.

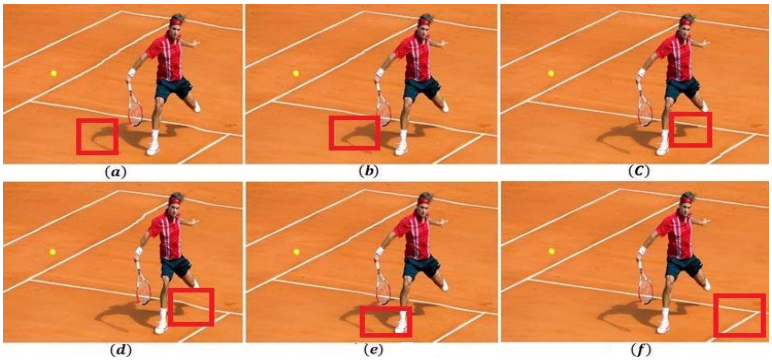

Figure 13. (a) SC; **(b)** SM; **(c)** SNS; **(d)** Warp; **(e)** Multi-Op; **(f)** proposed[47].

5) Category 5

The distortion of shadow structures in the image is seen in **Figure 14**. From the obtained results it is analyzed that the warp operator generates fewer distortions when the shadow regions are dominant in the images. However, SM and SNS produce a considerable number of distortions as compared to Multi-Op, SC, and the proposed framework. In the category-5 image type, the proposed framework produces a considerable percentage of distortion. **Figure 15** shows the clustering of the retargeting operators that produce a similar types of results. For category-1 image types two clusters are formed based on the percentage of distortion. Cluster-1 comprises SM and Warp operators while cluster-2 contains SNS and Multi-Op. For the category-2 image type only one cluster is formed which contains Warp and Multi-Op. Similarly, for category-3 image types, two clusters are formed. The first cluster contains SM and Multi-Op operators, while another cluster comprises SC and SNS operators. Multi-Op operators yield comparable outcomes in category-4. For the category-4 image type, two clusters are formed. The first cluster contains SC and SM operators while the other cluster presents Warp and Multi-Op. Lastly, for the category-5 image type only one cluster is formed which contains SM and SNS image retargeting operators. The Multi-Op approach works well for category (3 & 4)

images but fails when it is applied for categories 1, 2, and 4 image types. The proposed framework performs well for all the categories of images except category-5.

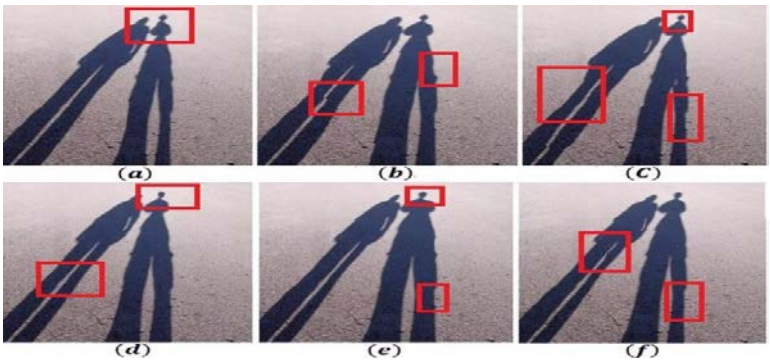

Figure 14. (a) SC; **(b)** SM; **(c)** SNS; **(d)** Warp; **(e)** Multi-Op; **(f)** proposed[47].

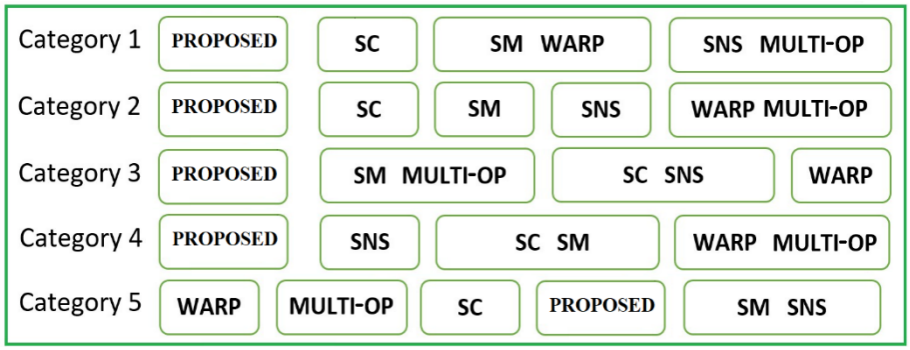

Figure 15. Comparison of results based on different categories of image.

The performance of the proposed framework is impeded in category-5 image. The existence of shadows as dominant objects in the image is the primary cause of distortion. The visible shadow areas are highly dominant in the image. The proposed framework may not perform well as deformations in the retargeted image may be noticeable to the human eye. Another cause of structural distortion is the presence of less variance in the foreground and background areas. Since shadow and background regions have comparable colour compositions, optimal seams can travel through shadow regions to choose the least energy pixels. As a result, selecting pixels from shadow regions to build appropriate seam routes might cause ROI distortion. More other types of images might be considered with many other image properties to justify the performance of the proposed framework. Unfortunately, because to space limitations, only a subset of the data is examined and given in the study.

7.2. Image expansion

In the proposed work, SIDR algorithm is also capable to apply image enlargement operation on the images. The ideal seams that are eliminated during image shrinking operations are again artificially inserted at different locations in the image. To enlarge the size of the image the location of the least energy pixels are preserved in one dimensional array which are eliminated during image shirking operation. In the process of image enlargement these locations are traced to form an optimal seam which is further inserted to expend the size of the image. In image enlargement, the replication procedure causes image stretching which can generate image artifacts. To get superior image enlargement outcomes, it is critical to strike a balance between the image's conspicuous portion and the artificially added section. For downsampling and expansion, a 500 × 355 resolution input image is used. The entire image enlargement process that is carried out by the proposed algorithm is shown in **Figure 16**.

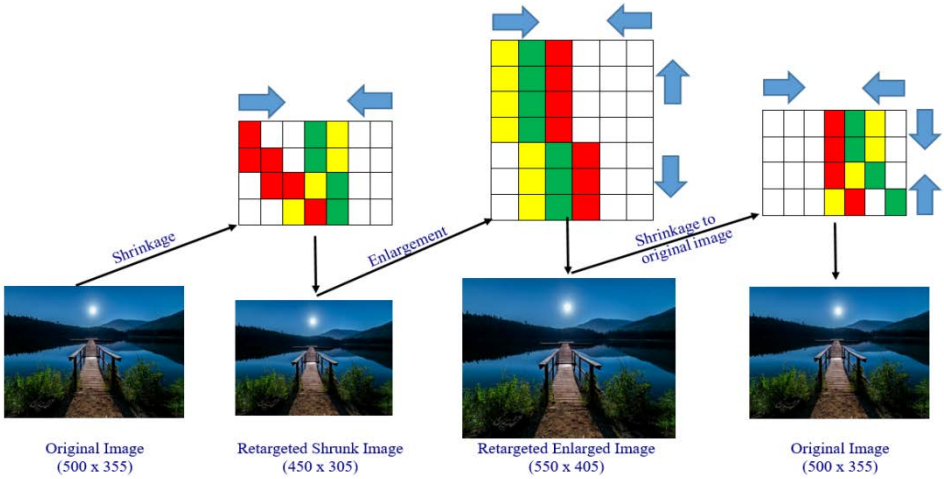

Figure 16. Down-sampling and enlargement of a single image multiple time using the proposed framework[50].

In the seam elimination procedure the proposed technique identifies the best seam paths. The entire image enlargement process may be seen as a process of going back in time to recover pixels from a larger image that would have been deleted by seam removals operation. In **Figure 16**, flowchart is shown to depict the process of both image shrinking and enlargement.

7.3. Percentage distortion analysis

The structural similarity index (SSIM) may determine the degree of visual resemblance between two input images[51,52]. The SSIM outperforms the Mean-Square Error (MSE) and Peak Signal-to-Noise-Ratio (PSNR). The structural information of the items in the image is interpreted by SSIM. Nearby pixels have a significant influence on the structural information of an image. When a source image is retargeted using any known retargeting method, the local and global maps convey substantial information about the variance in the source image. The similarity indices are then modified to provide the deformation percentage, as shown in **Figure 17**. **Figure 17** indicates that the suggested framework's retargeted results produces the least degree of deformation and suitable for all the chosen categories of images excluding category-5.

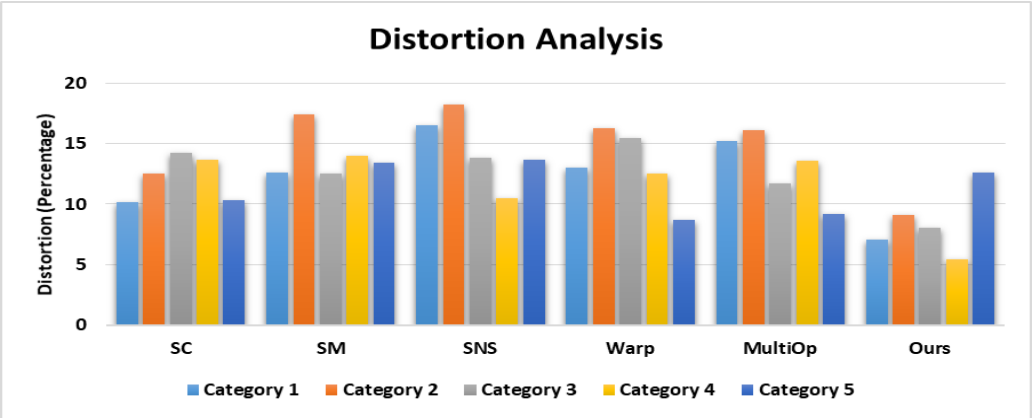

Figure 17. Comparative analysis of percentage distortion in different techniques.

The Warp approach produces the best results for category-5 images, in which the shadow is the sole notable item in the image. The suggested framework performs poorly on the category-5 image type, as described in section 5. The main reason of found due to less energy fluctuation in category-5 image. The ideal seams formed by the SDIR algorithm cover the pixels in the shadow and background areas. As compared to the existing techniques the suggested framework produces good results for image that are considered in categories 1, 2, 3, and 4.

7.4. Average percentage of distortion

The comparison of various strategies based on average distortion is shown in **Figure 18a**. It is obvious that the suggested framework has the lowest distortion values for all selected categories of images. **Figure 18b** depicts a comparison of average distortion. The percentage distortion values from all other methodologies other than the suggested framework are averaged, compared, and expressed according to the type of images.

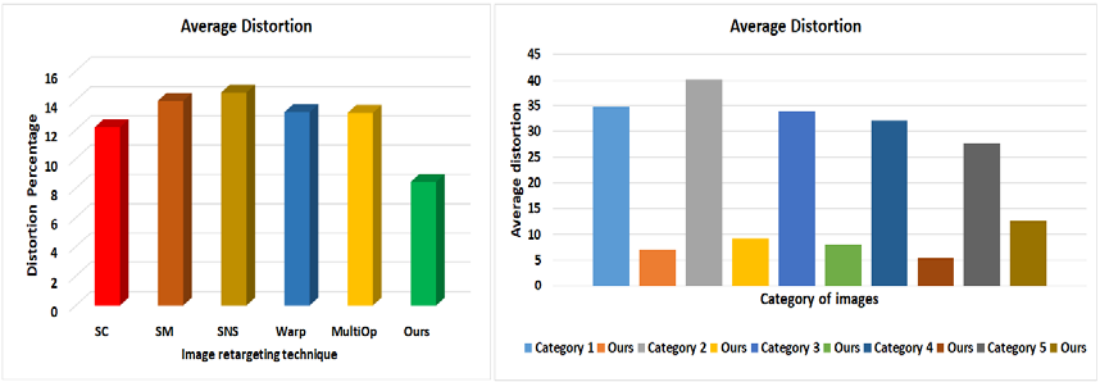

(a) **(b)**

Figure 18. Comparison of average percentage distortion.

Figure 18b presents that the suggested framework produces superior outcomes for all image types except category-5. The main reason for high deformation is the existence of shadow as a conspicuous item in the image that covers a substantial area. The results obtained by the proposed framework can be influenced by two major factors such as (i) when the shadow regions are dominant in the image; (ii) less intensity fluctuation in the background and foreground regions. The viewer can see high structural deformation in the image while the aforementioned two factors are extremely involved in the image.

8. Conclusions

The effectiveness of the saliency map influences the results of image retargeting algorithms. The different existing state-of-the-art cause distortions on significant portions of the image and do not treat shadow as a prominent image structure. After conducting several studies, the researchers determined that shadow objects may also be viewed as informational content of the image that draws the human eye to the primary items of the image. Because of the presence of shadows, the viewer can comprehend important contents such as the intensity of the incident light on the objects, the depth of the object, the angle of the incident light, and other critical elements of the objects. As a result, it is critical to keep the object's shadow while retargeting images. This research proposes a shadow-preserving image resizing system in which the saliency map is initially derived via segmentation. The extracted saliency map's correctness is evaluated quantitatively. The shadow map is extracted from the suggested shadow map framework, which executes a series of image pre-processing procedures. Ultimately, the various maps are integrated to provide an efficient significance map. To improve the image retargeting process, the extracted significance map is fed into the SDIR technique to retarget the images. The existing SDIR technique utilizes the proposed framework to highlight salient objects and shadow regions as prominent structures and limit the seams to cover them. The suggested framework's efficiency is demonstrated by comparing the results with existing image resizing algorithms. As compared to the current state of the art, the suggested framework achieves remarkable results in terms of low distortion percentage. The comparative findings show that, except for category-5, the suggested framework produced better outcomes in all image types. The fundamental reason for the proposed framework's failure is that if an image includes shadow areas that cover a considerable portion of the image and background pixels with very little intensity change, there may be distortions in the retargeted image that are extremely visible to the human eye.

Author contributions

Conceptualization, AG and AA; methodology, AG; software, AG; validation, AG, AA and PK; formal analysis, AG; investigation, AG; resources, AG; data curation, AG; writing—original draft preparation, AG and AA; writing—review and editing, AG, AA and PK; visualization, AG; supervision, AG, AA and PK; project administration, AG. All authors have read and agreed to the published version of the manuscript.

Conflict of interest

The authors declare no conflict of interest.

References

1. Vaquero D, Turk M, Pulli K, et al. A survey of image retargeting techniques. *Applications of Digital Image Processing XXXIII* 2010; 7798: 779814. doi: 10.1117/12.862419
2. Wei Y, Wen F, Zhu W, Sun J. Geodesic saliency using background priors. In: Fitzgibbon A, Lazebnik S, Perona P, et al. (editors). *Computer Vision—ECCV 2012*, Proceedings of 12th European Conference on Computer Vision; 7–13 October 2012; Florence, Italy. Springer; 2012. pp. 29–42.
3. Itti L, Koch C, Niebur E. A model of saliency-based visual attention for rapid scene analysis. *IEEE Transactions on Pattern Analysis and Machine Intelligence* 1998; 20(11): 1254–1259. doi: 10.1109/34.730558
4. Stentiford FWM. Attention-based image similarity measure with application to content-based information retrieval. *Storage and Retrieval for Media Databases* 2003; 5021: 221–232. doi: 10.1117/12.476255
5. Santella A, Agrawala M, DeCarlo D, et al. Gaze-based interaction for semi-automatic photo cropping. In: Proceedings of the SIGCHI Conference on Human Factors in Computing Systems; 22–27 April 2006; Montréal, Québec, Canada.
6. Gal R, Sorkine O, Cohen-Or D. Feature-aware texturing. In: Proceedings of the Eurographics Symposium on Rendering Techniques; 2006; Nicosia, Cyprus. pp. 297–303.
7. Golub E. PhotoCropr: A first step towards computer-supported automatic generation of photographically interesting cropping suggestions. Available online: https://www.yumpu.com/en/document/read/45331521/a-first-step-towards-computer-supported-automatic-generation-of- (accessed on 20 August 2023).
8. Liu F, Gleicher M. Automatic image retargeting with fisheye-view warping. In: Proceedings of the 18th Annual ACM Symposium on User Interface Software and Technology; 23–26 October 2005; Seattle, WA, USA. pp. 153–162.
9. Guo Y, Liu F, Shi J, et al. Image retargeting using mesh parametrization. *IEEE Transactions on Multimedia* 2009; 11(5): 856–867. doi: 10.1109/TMM.2009.2021781
10. Sachdeva S, Ali A, Khalid S. Telemedicine in healthcare system: A discussion regarding several practices. In: Choudhury T, Katal A, Um JS, et al. (editors). *Telemedicine: The Computer Transformation of Healthcare*. Springer Cham; 2022. pp. 295–310.
11. Sachdeva S, Ali A. Advanced approach using deep learning for healthcare data analysis in IOT system. In: Marriwala N, Tripathi CC, Jain S, et al. (editors). *Emergent Converging Technologies and Biomedical Systems*, Proceedings of ETBS 2021. Springer Singapore; 2022. pp. 163–172.
12. Sachdeva S, Ali A. Machine learning with digital forensics for attack classification in cloud network environment. *International Journal of System Assurance Engineering and Management* 2022; 13: 156–165. doi: 10.1007/s13198-021-01323-4
13. Chen J, Bai G, Liang S, Li Z. Automatic image cropping: A computational complexity study. In: Proceedings of 2016 IEEE Conference on Computer Vision and Pattern Recognition (CVPR); 27–30 June 2016; Las Vegas, NV, USA. pp. 507–515.
14. Kao Y, He R, Huang K. Automatic image cropping with aesthetic map and gradient energy map. In: Proceedings of 2017 IEEE International Conference on Acoustics, Speech and Signal Processing (ICASSP); 5–9 March 2017; New Orleans, LA, USA. pp. 1982–1986.
15. Guo G, Wang H, Shen C, et al. Automatic image cropping for visual aesthetic enhancement using deep neural networks and cascaded regression. *IEEE Transactions on Multimedia* 2018; 20(8): 2073–2085. doi: 10.1109/TMM.2018.2794262
16. Rahman Z, Pu YF, Aamir M, Ullah F. A framework for fast automatic image cropping based on deep saliency map detection and gaussian filter. *International Journal of Computers and Applications* 2019; 41(3): 207–217. doi: 10.1080/1206212X.2017.1422358
17. Garg A, Negi A. A survey on content aware image resizing methods. *KSII Transactions on Internet and Information Systems (TIIS)* 2020; 14(7): 2997–3017. doi: 10.3837/tiis.2020.07.015
18. Jiang W, Xu H, Chen G, et al. An improved edge-adaptive image scaling algorithm. In: Proceedings of 2009 IEEE 8th International Conference on ASIC; 20–23 October 2009; Changsha, China. pp. 895–897.

19. Liang Y, Su Z, Luo X. Patchwise scaling method for content-aware image resizing. *Signal Processing* 2012; 92(5): 1243–1257. doi: 10.1016/j.sigpro.2011.11.018
20. Pritch Y, Kav-Venaki E, Peleg S. Shift-map image editing. In: Proceedings of 2009 IEEE 12th International Conference on Computer Vision; 29 September–2 October 2009; Kyoto, Japan. pp. 151–158.
21. Avidan S, Shamir A. Seam carving for content-aware image resizing. *ACM Transactions on Graphics (TOG)* 2007; 26(3): 10-es. doi: 10.1145/1276377.1276390
22. Choi J, Kim C. Sparse seam-carving for structure preserving image retargeting. *Journal of Signal Processing Systems* 2016; 85: 275–283. doi: 10.1007/s11265-015-1084-3
23. Lin W, Zhang F, Lian R, et al. Seam carving algorithm based on saliency. In: Pan JS, Wu TY, Zhao Y, et al. (editors). *Advances in Smart Vehicular Technology, Transportation, Communication and Applications*, Proceedings of the First International Conference on Smart Vehicular Technology, Transportation, Communication and Applications; 6–8 November 2017; Kaohsiung, Taiwan. Springer Cham; 2017. pp. 282–291.
24. Li C, Hu R, Liang C, et al. Faster seam carving for video retargeting. In: Proceedings of 2018 25th IEEE International Conference on Image Processing (ICIP); 7–10 October 2018; Athens, Greece. pp. 823–827.
25. Patel D, Raman S. Accelerated seam carving for image retargeting. *IET Image Processing* 2019; 13(6): 885–895. doi: 10.1049/iet-ipr.2018.5283
26. Garg A, Negi A, Jindal P. Structure preservation of image using an efficient content-aware image retargeting technique. *Signal, Image and Video Processing* 2021; 15(1): 185–193. doi: 10.1007/s11760-020-01736-x
27. Garg A, Nayyar A, Singh AK. Improved seam carving for structure preservation using efficient energy function. *Multimedia Tools and Applications* 2022; 81(9): 12883–12924. doi: 10.1007/s11042-022-12003-1
28. Garg A, Singh AK. Analysis of seam carving technique: Limitations, improvements and possible solutions. *The Visual Computer* 2023; 39: 2683–2709. doi: 10.1007/s00371-022-02486-2
29. Kaufmann P, Wang O, Sorkine-Hornung A, et al. Finite element image warping. *Computer Graphics Forum* 2013; 32: 31–39. doi: 10.1111/cgf.12023
30. Li B, Duan LY, Lin CW, et al. Depth-preserving warping for stereo image retargeting. *IEEE Transactions on Image Processing* 2015; 24(9): 2811–2826. doi: 10.1109/TIP.2015.2431441
31. Del Gallego NP, Ilao J. Multiple-image super-resolution on mobile devices: An image warping approach. *EURASIP Journal on Image and Video Processing* 2017; 2017: 8. doi: 10.1186/s13640-016-0156-z
32. Islam MB, Wong LK, Low KL, Wong CO. Warping-based stereoscopic 3D video retargeting with depth remapping. In: Proceedings of 2019 IEEE Winter Conference on Applications of Computer Vision (WACV); 7–11 January 2019; Waikoloa, HI, USA. pp. 1655–1663.
33. Niu Y, Liu F, Li X, Gleicher M. Image resizing via non-homogeneous warping. *Multimedia Tools and Applications* 2012; 56(3): 485–508. doi: 10.1007/s11042-010-0613-0
34. Wang YS, Tai CL, Sorkine O, Lee TY. Optimized scale-and-stretch for image resizing. *ACM Transactions on Graphics* 2008; 27(5): 1–8. doi: 10.1145/1409060.1409071
35. Rubinstein M, Shamir A, Avidan S. Multi-operator media retargeting. *ACM Transactions on Graphics* 2009; 28(3): 1–11. doi: 10.1145/1531326.1531329
36. Su PC, Xiang ZH, Wu HW. SCAN: A multi-operator image retargeting scheme. In: Proceedings of Signal and Information Processing Association Annual Summit and Conference (APSIPA); 9–12 December 2014; Siem Reap, Cambodia. pp. 1–5.
37. Tsai WJ, Chen CF. Hybrid image retargeting. In: Proceedings of 2015 Visual Communications and Image Processing (VCIP); 13–16 December 2015; Singapore. pp. 1–4.
38. Zhu L, Chen Z, Chen X, Liao N. Saliency & structure preserving multi-operator image retargeting. In: Proceedings of 2016 IEEE International Conference on Acoustics, Speech and Signal Processing (ICASSP); 20–25 March 2016; Shanghai, China. pp. 1706–1710.
39. Garg A, Negi A. Structure preservation in content-aware image retargeting using multi-operator. *IET Image Processing* 2020; 14(13): 2965–2975. doi: 10.1049/iet-ipr.2019.1032
40. Karni Z, Freedman D, Gotsman C. Energy-based image deformation. *Computer Graphics Forum* 2009; 28(5): 1257–1268. doi: 10.1111/j.1467-8659.2009.01503.x
41. Chen R, Freedman D, Karni Z, et al. Content-aware image resizing by quadratic programming. In: Proceedings of 2010 IEEE Computer Society Conference on Computer Vision and Pattern Recognition-Workshops; 13–18 June 2010; San Francisco, CA, USA. pp. 1–8.
42. Shi M, Yang L, Peng G, Xu D. A content-aware image resizing method with prominent object size adjusted. In: Proceedings of the 17th ACM Symposium on Virtual Reality Software and Technology; 22–24 November 2010; Hong Kong, China. pp. 175–176.
43. Arbelaez P, Maire M, Fowlkes C, Malik J. Contour detection and hierarchical image segmentation. *IEEE Transactions on Pattern Analysis and Machine Intelligence* 2010; 33(5): 898–916. doi: 10.1109/TPAMI.2010.161
44. Available online: https://people.csail.mit.edu/mrub/retargetme/ (accessed on 20 August 2023).
45. Rubinstein M, Gutierrez D, Sorkine O, Shamir A. A comparative study of image retargeting. *ACM Transactions on Graphics* 2010; 29(6): 1–10. doi: 10.1145/1882261.1866186

46. Margolin R, Zelnik-Manor L, Tal A. How to evaluate foreground maps? In: Proceedings of 2014 IEEE Conference on Computer Vision and Pattern Recognition; 23–28 June 2014; Columbus, OH, USA. pp. 248–255.
47. Available online: https://www3.cs.stonybrook.edu/~minhhoai/projects/shadow.html (accessed on 20 August 2023).
48. Vicente TFY, Hou L, Yu CP, et al. Large-scale training of shadow detectors with noisily-annotated shadow examples. In: Leibe B, Matas J, Sebe N, et al. (editors). *Computer Vision—ECCV 2016*, Proceedings of 14th European Conference; 11–14 October 2016; Amsterdam, Netherlands. Springer Cham; 2016. pp. 816–832.
49. Abhayadev M, Santha T. Multi-operator content aware image retargeting on natural images. *Journal of Scientific & Industrial Research* 2019; 78: 193–198.
50. Available online: https://pixabay.com/ (accessed on 20 August 2023).
51. Garg A, Singh AK. Performance analysis of seam diversion based image retargeting technique based on edge detection operators. *Multimedia Tools and Applications* 2023; 82: 23207–23250. doi: 10.1007/s11042-022-14157-4
52. Garg A. Content-aware image retargeting technique and iterated function system: Frameworks, applications, and possible future advancements. *Multimedia Tools and Applications* 2023; 1–45. doi: 10.1007/s11042-023-16348-z